19th Brazilian Congress of Thermal Sciences and Engineering
November 06th-10th, 2022, Bento Gonçalves - RS - Brazil

ENC-2022-0409
BOUDOUARD, REFORMING OF CHAR AND METHANATION REACTION EVALUATION BY CFD SIMULATIONS OF FLUIDIZED-BED REACTOR FOR GASIFICATION

Vitor Alberto Lemes Monteiro
Universidade Federal de Uberlândia, Faculdade de Engenharia Mecânica, Av. João Naves de Ávila, 2121, 38408-100, Uberlândia-MG.
vitoralbertolemes@hotmail.com

Alam Gustavo Trovó
Universidade Federal de Uberlândia, Instituto de Química, Av. João Naves de Ávila, 2121, 38400-902, Uberlândia-MG.
alamtrovo@ufu.br

Marcelo Braga dos Santos
Universidade Federal de Uberlândia, Faculdade de Engenharia Mecânica, Av. João Naves de Ávila, 2121, 38408-100, Uberlândia-MG.
marcelo.bragadossantos@ufu.br

Solidônio Rodrigues de Carvalho
Universidade Federal de Uberlândia, Faculdade de Engenharia Mecânica, Av. João Naves de Ávila, 2121, 38408-100, Uberlândia-MG.
solidonio@ufu.br

Abstract. *The gasification in fluidized-bed reactor is an important subject related to Waste to Energy systems. There are still no ready solutions for fast and reliable simulations in designing or controlling such units. In this context, the objective of this work is to develop a model to evaluate some heterogeneous reactions among the subprocesses of the gasification operation. Such reactions are part of the thermal degradation of biomass and are quite especial due to its phase conversion, from solid to gas. The Eulerian-Eulerian approach was applied using OpenFOAM software to a computational fluid dynamic system to simulate Boudouard, Reforming of Char and Methanation reactions. A bubbling fluidized-bed reactor containing silica sand as bed material was modelled with a determined gas injection (CO_2, H_2O and H_2) for the simulation of such gasification subprocesses of a generic carbonaceous biomass. The results show quantitively consistent progression of thermal degradation process in terms of biomass solid phase transformations into gas of each chemical reaction separately. Also, the Reacting Zone could be determined and better analysed. This detailed evaluation of such reactions was important for the authors research line studies, which includes a development of a large-scale gasifier of municipal refuse-derived fuel in fluidized bed.*

Keywords: *devolatilization, heterogeneous reactions, renewable energy, bubbling fluidized bed, multiphase flow*

1. INTRODUCTION

The line of research of our group is within the scope of WTE technologies and consists of the study of a semi-industrial scale fluidized bed gasification plant to convert municipal solid waste (MSW) into energy. Previously study have demonstrated a solid waste processing line (SWPL) to produce the municipal refuse-derived fuel (MRDF) biomass from MSW (Infiesta et al., 2019). Such fluidized bed gasification reactor, capable of recovering syngas from MRDF, was developed in experimental basis by our research group. The future perspective is to develop a full Computational Fluid-Dynamics (CFD) model to reproduce such reactor process and to improve this WTE gasification technology.

The objective of this paper is to implement some heterogeneous reactions in a computational model, evaluating the conversion of solid particles into gaseous phase.

2. MATERIALS AND METHODS

The development of the mentioned semi-industrial scale gasifier model consists of some computational procedures implemented into OpenFOAM 8 software. The gasification process was represented by some sub-processes (Figure 1) involving the devolatilization, drying, homogeneous and heterogeneous reactions. The final product of the reactor is the conversion of the solid biomass in a combustible gas, named syngas.

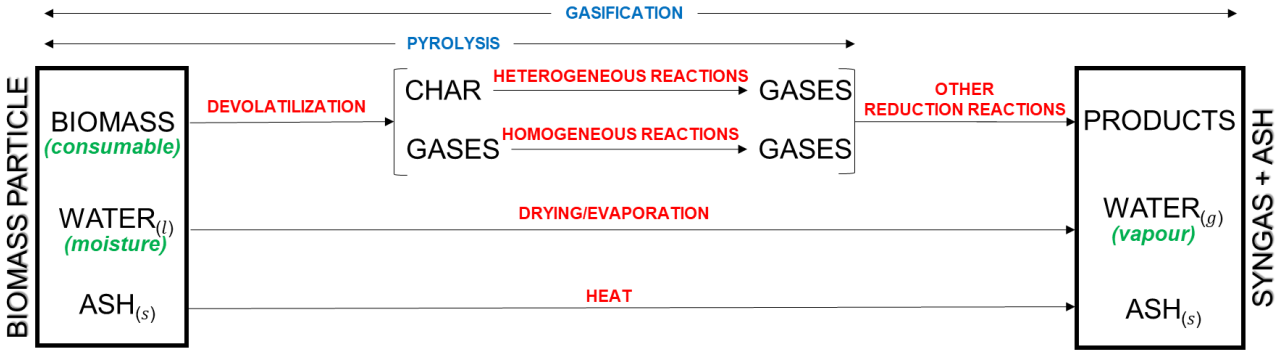

Figure 1. Biomass gasification modeling steps.

In the present work, the reactor's geometry was simplified, and its dimensions were reduced to evaluate the heterogeneous reactions of biomass (Figure 2). This way, the control of the reactions can provide clear results to evaluate correctly each reaction.

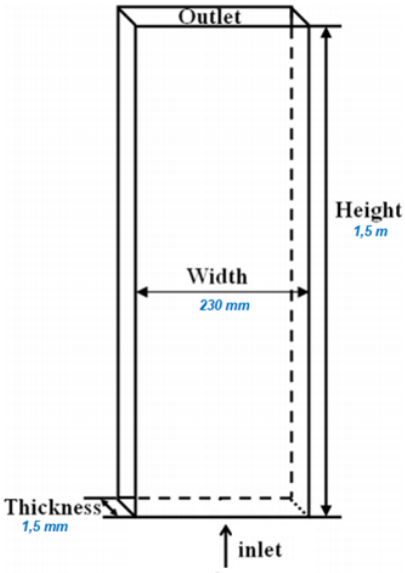

Figure 2. Simplified geometry of the reactor implemented (Adapted from Ku, Li and Løvås, 2015)

This CFD system consists of three parts: gas phase, biomass particles and silica sand, last ones are two solid phases. The biomass particles were considered as a full carbon phase and gas phase has all the gaseous species considered: H_2O, CO_2, CO, H_2, O_2, N_2 and CH_4. The heterogeneous reactions analyzed in this paper are the reaction of a gaseous specie with the solid carbon, producing only gaseous species. Therefore, for each reaction simulation, the inlet gas implemented were 100% of the reagent gas of such reaction (i.e. CO_2, H_2O or H_2).

2.1 Governing Equations

The Eulerian-Eulerian approach solves the governing equations for each phase, in which the sum of the volumetric particle fraction of the different phases is always unit. The governing equations for each phase were implemented as the computational methodology properly detailed by Rusche (2002) and are briefly presented below.

The mass balance equation is written as:

$$\frac{\partial}{\partial t}\alpha_k\rho_k + \frac{\partial}{\partial x_i}\alpha_k\rho_k U_k = \dot{m}_k + \dot{m}_{p\to k}, \quad (1)$$

The momentum equations are,

$$\frac{\partial}{\partial t}(\alpha_k \rho_k U_k) + \nabla \cdot (\alpha_k \rho_k U_k U_k) = \alpha_k \rho_k g_i + \nabla \cdot S_k + I_k, \quad (2)$$

$$S_k = \nabla \cdot (\alpha_k \tau_k) - \alpha_k \nabla p - \nabla p_k, \quad (3)$$

$$\tau_k = \mu_{eff} \frac{1}{2} [\nabla U_k + \nabla U_k^T] + \left(\lambda_k - \frac{2}{3}\mu_{eff}\right)(\nabla \cdot U_k) I, \quad (4)$$

Energy balance equation is given as,

$$\frac{\partial}{\partial t}(\alpha_k \rho_k E_k) + \nabla \cdot (\alpha_k \rho_k U_k E_k) = \alpha_k \left(\frac{\partial p}{\partial t} + U_k \cdot \nabla p\right) - \nabla\left(\alpha_k \kappa_{eff} \nabla T_k\right) + \phi + A_{sp} h (T^* - T_k) + \dot{q}_k, \quad (5)$$

The subindex k indicates the solid or the fluid phase, e.g. for the particles present into solid phase fraction (α_k) was written as α_p, the one of the gas continuous phases as α_g. The index i represents each one of the species present into solid or gas phase. In these equations, α_k is the volume fraction, ρ_k the density and U_k the velocity of the respective phase. $\dot{m}_k$ is the mass source term and $\dot{m}_{p \to i,k}$ is the interphase mass transfer term from converted biomass particle (p) products into gas phase.

The momentum equation defines S_k as the k-phase stress tensor, p the pressure, p_k the granular pressure when solid phase, λ_k the solid bulk viscosity and I_k is the momentum exchange term which may include drag forces, turbulent dispersion, between others.

k_{eff} & μ_{eff} represents the effective thermal conductive and viscosity respectively, which also includes the turbulent effects.

At the energy transport equation, ϕ is the viscous dissipation and E_k the enthalpy, A_{sp} is the superficial area per volume unit of the particle phase, h is the convective coefficient and T^* is the temperature of the exchange phase and $\dot{q}_k$ the heat source term of the k-phase.

The drag model is written as combination of the Ergun Equation (Ergun, 1952) and Wen and Yu drag model (Wen and Yu, 1966). The drag factor is one for a spherical particle given by Schiller & Naumann (1935). The combination of the two drag models leads to Gidaspow's Drag Model (Gidaspow, 1994). The Gidaspow's Drag Model is recommended for dense particulate flow, as one find in this type of reactor (Zhong et al., 2016).

Empirical correlation used for calculating the Nusselt's number (Ranz and Marshall, 1952) for heat flux between phases are:

$$Nu = 2 + 0.6 Re^{0.5} \mathrm{Pr}^{0.33}, \quad (6)$$

$$Nu = \frac{h d_p}{\kappa}, \quad (7)$$

Using Eq. (6), the convective coefficient (h) for the energy transport equation (Eq. 5) is estimated. The Sutherlands's transport model (Sutherland, 1893) evaluates dynamic viscosity (μ) as function of temperature (T) of a specific coefficient (A_s) and of the Sutherland Temperature (T_s) as follow:

$$\mu = \frac{A_s \sqrt{T}}{1 + \frac{T_s}{T}}, \quad (8)$$

JANAF Thermochemical Tables (Chase, 1998) provides the coefficients of a polynomial relation to calculate the specific heat (c_p) as function of temperature (T).

The balance of mass fraction species (Y) is written as:

$$\frac{\partial}{\partial t}\left(\alpha_k \rho_k Y_{i,k}\right) + \nabla \cdot \left(\alpha_k \rho_k U_k Y_{i,k}\right) = \nabla\left(\alpha_k \rho_k \mathrm{D}_{\mathrm{eff}} \nabla Y_{i,k}\right) + \dot{m}_{p \to i,k}, \quad (9)$$

where D_{eff} is the effective mass diffusivity of ith-specie and the terms $\dot{m}_{p \to i,k}$ represents the mass conversion (consumption or generation) of carbonaceous particles into ith-specie of k-phase. In this work, once the solid biomass particle phase if modeled with one species (char), there is only conversion of the solid char into gas.

2.2 Heterogeneous Reactions

As mentioned in the Figure 1, the reactions implemented into software, which are part of the heterogeneous balanced reactions of the gasification process, are:

$$C_{(s)} + CO_{2(g)} \rightarrow 2CO_{(g)} \qquad \Delta H = 172\ kJ/mole \tag{10}$$

$$C_{(s)} + H_2O_{(g)} \rightarrow CO_{(g)} + H_{2(g)} \qquad \Delta H = 131\ kJ/mole \tag{11}$$

$$C_{(s)} + 2H_{2(g)} \rightarrow CH_{4(g)} \qquad \Delta H = -75\ kJ/mole \tag{12}$$

The Eq. (10) is the Boudouard reaction, the Eq. (11) is the reforming of the char, the Eq. (12) is the methanation reaction, also called by some authors hydrogasification reaction. The thermal energy (ΔH) required described by (Hasse et al., 2021), was implement to each reaction as a source term ($\dot{q_k}$) into the energy balance equation (eq. 5)

The char consumption rate by each heterogeneous reaction (R_{het}) is given by:

$$R_{het} = \frac{R_{kin}R_{diff}}{R_{kin}+R_{diff}}P_i \tag{13}$$

where R_{diff} and R_{kin} are the diffusion rate and kinetic rate, respectively, P_i is the partial pressure of the specie (H_2O, CO_2 or H_2). And those rates are written as the equations (14) and (15) below:

$$R_{kin} = -AT^{\beta}\left(-\frac{E_a}{RT_p}\right) \tag{14}$$

where E_a is the activation energy, A is the frequency factor, β is the temperature exponent, which in this case is set to unity, T_p the temperature of the particle and R is the gas constant.

$$R_{diff} = \frac{C_i\left[\frac{T_p+T_g}{2}\right]^{0.75}}{d_p} \tag{15}$$

where Ci is the mass diffusion rate constant, T_p and T_g the temperature of the particle and the gas, respectively, d_p the particle diameter, which is calculated by:

$$d_p = \left(\frac{6m_p}{\pi\rho_p}\right)^{\frac{1}{3}} \tag{16}$$

The parameters of the equation (14) and (15) are defined experimentally for each chemical reaction (Table 1).

Table 1. Rate constants for the heterogeneous reactions (Klimanek and Bigda, 2018).

Reaction	A [s/m]	E_a [J/kmol]	C [sK$^{-0.75}$]
Boudouard	2.0×10^{-7}	7.9×10^{7}	5×10^{-12}
Reforming of Char	2.0×10^{-7}	7.9×10^{7}	5×10^{-12}
Methanation	1.18×10^{-5}	1.49×10^{8}	5×10^{-12}

Therefore, the mass conversion contributions ($\dot{m}_{p\rightarrow i,k}$) are written in terms of the coefficients (n_i) of each element from each reaction (Eq. 10, 11 and 12):

$$\dot{m}_{p\rightarrow i,k} = n_i\left(\alpha_p\rho_p Y_{char}\right)R_{het} \tag{17}$$

where R_{het} is specific for each reaction (Boudouard, reforming of char or methanation), Y_{char} represent the volumetric fraction of char from biomass particle.

In this model, the particle diameter shrinkage was not considered, so that this parameter remains constant over time. However, the consumption of biomass is numerically implemented by the reduction of mass fraction of biomass particles by the consumption rate.

2.3 Configuration of bubbling fluidized bed reactor

As mentioned, the components of gaseous phase are H_2O, CO_2, CO, H_2, O_2, N_2 and CH_4. The biomass phase is composed of carbon. Simplified 2D geometry was set with 1.5 m of height and 0.15 m of width (Figure 2 and Figure 3a). This geometry has a pseudo 2D domain in which the software considers a small thickness to avoid numerical ill conditioning. This geometry was divided into squared cells of 7.5×10^{-3} m of edge, totaling 4000 hexahedral finite volume cells in the mesh grid (Figure 3b).

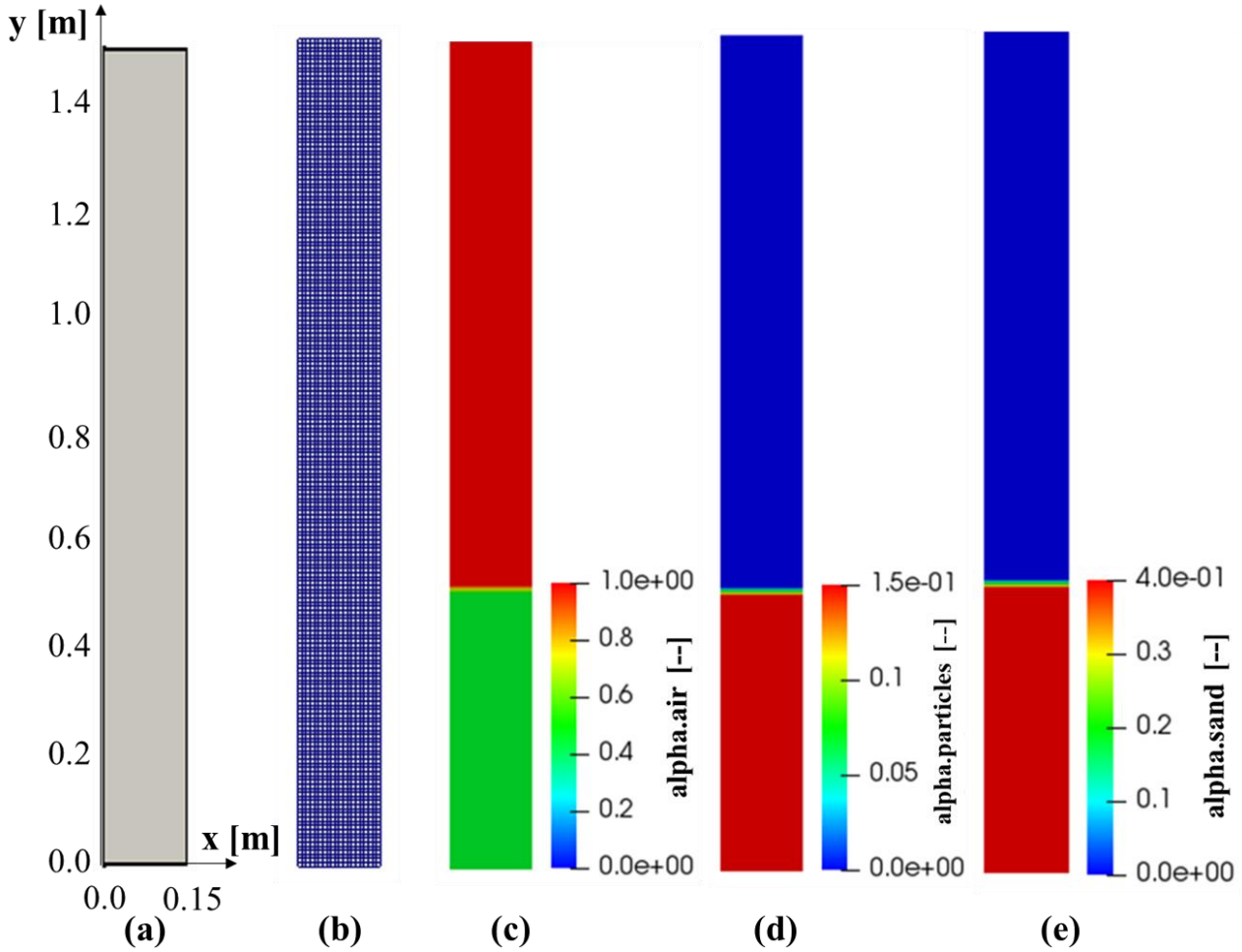

Figure 3. Representation of the (a) geometry, (b) mesh and initial conditions of (c) volume particle fractions of air, (d) particles and (e) sand phases.

The reactor was initially filled up to one third of its height with sand (Figure 3e) and biomass particles (Figure 3d), into a continuous medium of gas (Figure 3c). The total mass of biomass particle was 0.041 kg (100% carbonaceous matter) and 1.508 kg of sand, plus the gas media. Some other simulation parameters are showed at Table 2 and initial conditions at Figure 3.

A constant time step of 0.5×10^{-3} was implemented and total integration time adopted was 10 s. The last one is enough to observe significant thermal degradation of the char initial mass and production of gaseous components. Besides, 10 s was sufficient to stabilize the bubbling in the fluidized bed reactor, when the composition of the syngas (Figure 10) and the inlet pressure (Figure 12) remains constant.

Table 2. Initial conditions and other parameters.

Parameters	Value
Biomass feed rate [kg/h]	N/A
Biomass temperature [K]	670
Biomass Particle diameter [m]	0.75×10^{-3}
Biomass initial mass [kg]	0.041
Density of biomass (char) [kg/m³]	180
Energy source term [kg.m²/s³]	Eq. (10), (11) and (12)
Density of sand particles [kg/m³]	2500
Sand particles diameter [m]	0.25×10^{-3}
Initial bed temperature [K]	670
Operating temperature [K]	670
Gasifier walls condition	Insulated
Interstitial inlet velocity of air [m/s]	0.1
Outlet pressure [kPa]	Atmospheric
Atmospheric pressure [kPa]	100
Mesh grid square cells edge dimensions [m]	0.0075

N/A – not applied

3. RESULTS AND DISCUSSION

Figure 4 depicts the final state of the reactor at the end of the simulation time. The biomass particles, fully composed by char, different from the initial stage (Figure 3d), remains at the upper part of the bed of the reactor (Figure 4a) due to its specific mass. Whereas the silica sand (Figure 4b) was concentrated downwards. Once the chemical reactions implement in this model involves the consumption of the char, the region where the char particles are concentrated will characterize the main Reacting Zone (RZ) of the thermochemical reactor. This can be an important information of the functionality of the gasifier in terms of the chemical reactions: the char particles heat transfer could be affected, since the heat generated from exothermic reactions is transferred to the gas and released outside of reactor. This way, the thermal inertia of the reactor promoted by the sand region can be compromised. Ideally, the char particles should be homogeneously mixed with sand at the continuous operation of the equipment. However, the generation of thermal energy at this zone may improve the endothermic chemical reactions, as Methanation (Eq. 12), for example.

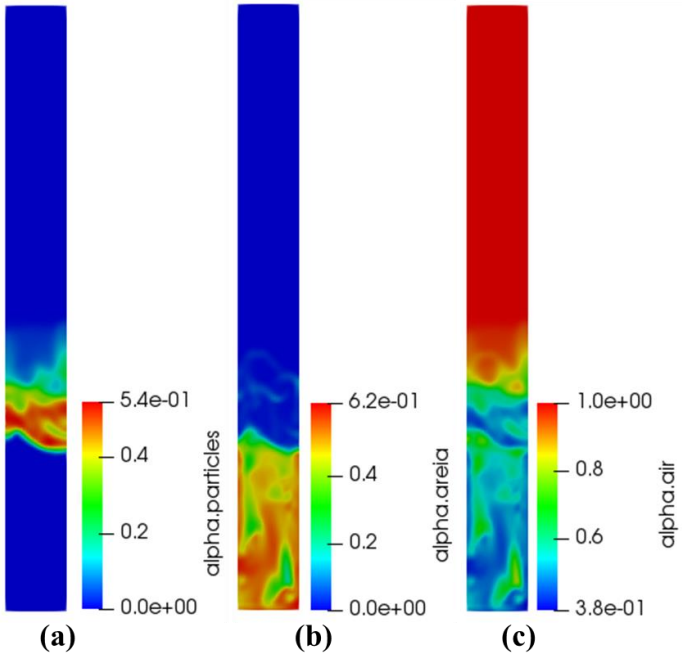

Figure 4. General aspect of the internal fluid-dynamics of the reactor of any reaction simulation in terms of (a) particles mass fraction, (b) sand mass fraction and (c) air mass fraction

As expected by the reactions from Eqs. (10), (11) and (12), respectively, related by Figs. 5, 6 and 7, all produced species of the syngas are increased with simulation time, whereas the insufflated one is reduced. For instance, at the Reforming of char reaction (Figure 6) there is the production of the CO and H_2 species and, consequently, the decrease of the H_2O within the reactor. The inlet insufflation of H_2O is constant, however, due to its chemical conversion, the amount of this component is decreased in the reactor.

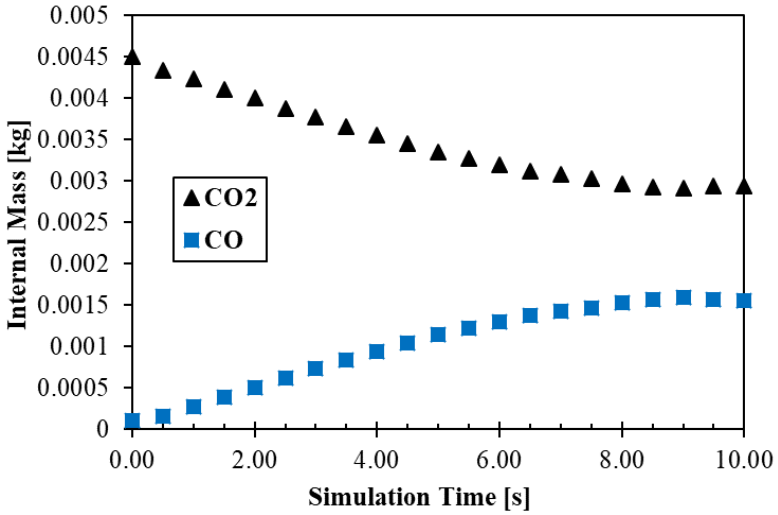

Figure 5. Running of composition of the gaseous species during simulation of Boudouard reaction

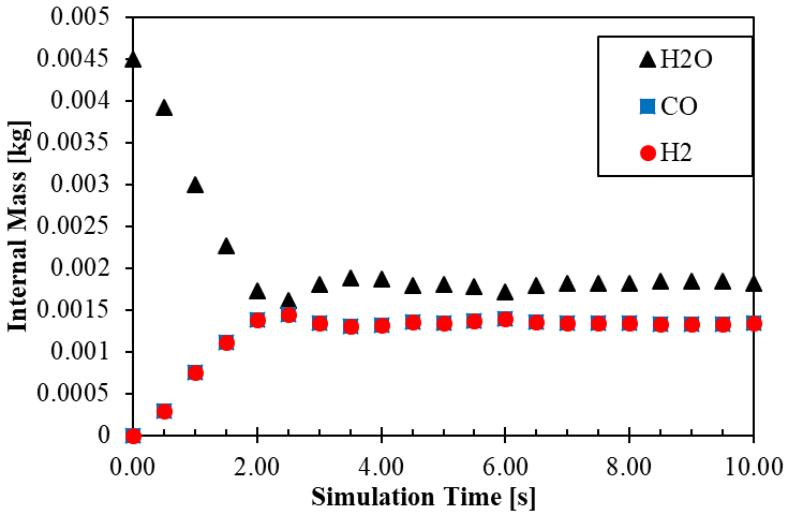

Figure 6. Running of composition of the gaseous species during simulation of Reforming of char reaction

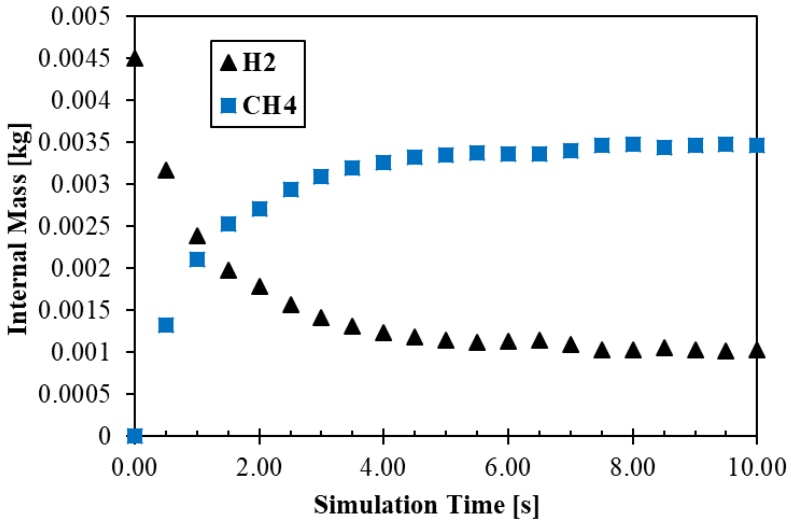

Figure 7. Running of composition of the gaseous species during simulation of Methanation of char reaction

Under the configurations of the reactor and some fixed parameters (Table 2), the char particles are consumed (Figure 8) and transferred from solid to gaseous phase in a constant rate, since the temperature of the reactor and chemical rates are constant. As showed to Reforming reaction (Figure 8), for Boudouard and Methanation reactions, similar char consumption rate was observed.

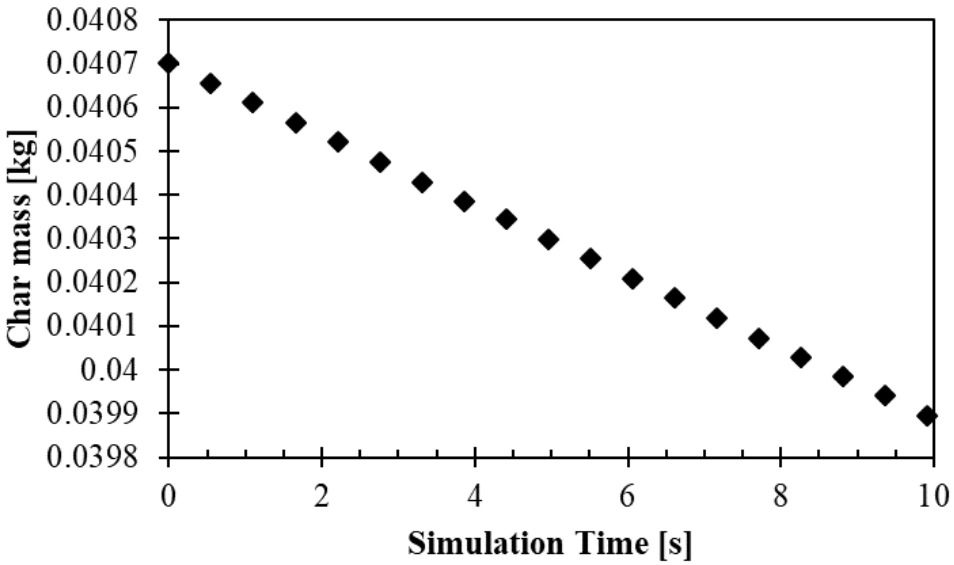

Figure 8. Char consumption during simulation time at Reforming of char reaction

All gaseous species are showed separately at the Figure 10 at the last time step of the simulation. Although all the implemented species are shown, the Reforming reaction not involves the components CO_2, O_2, N_2 and CH_4, for example. As mentioned, the higher concentration of the produced gases (Figure 10c and 7d), are near the char particles, at the upper part of the fluidized bed, enclosing the RZ. The reagent specie of H_2O insufflated into the bottom of the reactor is homogeneous until reach the RZ, where this component is diluted into the other produced components.

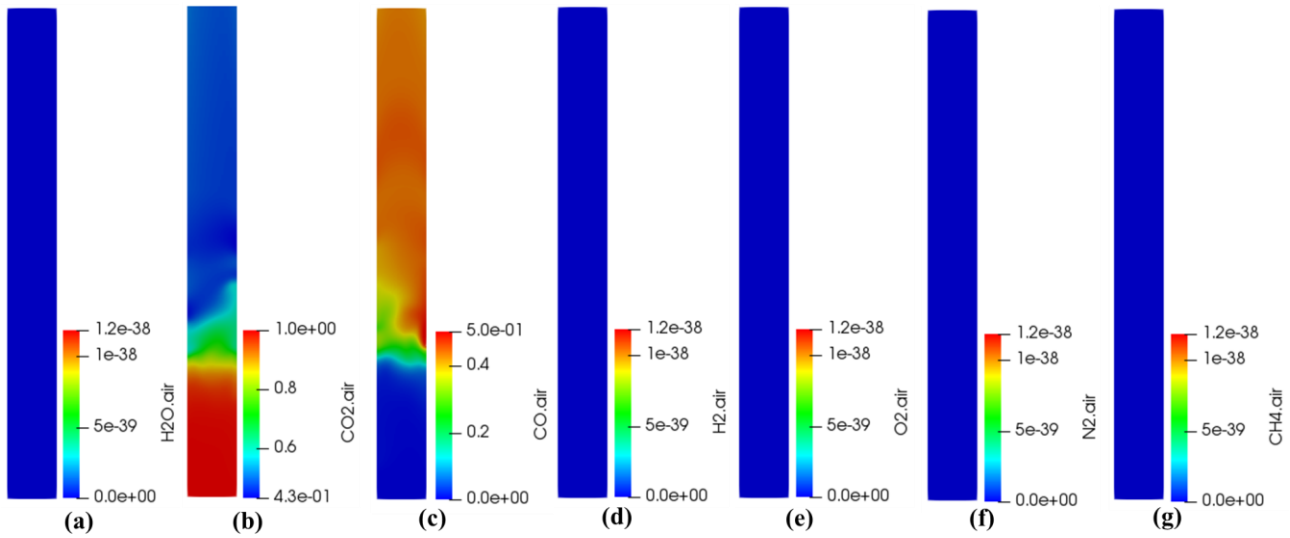

Figure 9. Final composition of the reactor at Boudouard reaction simulation. (a) H_2O, (b) CO_2, (c) CO, (d) H_2, (e) O_2, (f) N_2 and (g) CH_4.

After 2 s of simulation time, the system reaches a steady regime, which the bubbling fluid-dynamics has no significant changes, and inlet pressure remains stable (Figure 12). Although the fluid-dynamics remains at steady state, with no great variation within the flow, the chemical reactions did not follow the same pattern, for them were necessary approximately 10 s (Figure 5), 3 s (Figure 6) and 1.5 s (Figure 7) to obtain constant composition of syngas, respectively for Boudouard, Reforming of Char and Methanation reactions. Even if is possible to estimate when the thermal steady state is reached, it was not done. That information will be considered in future works, since it is important to the determine the minimum time to reach a continuous operating condition in semi-industrial scale gasifier.

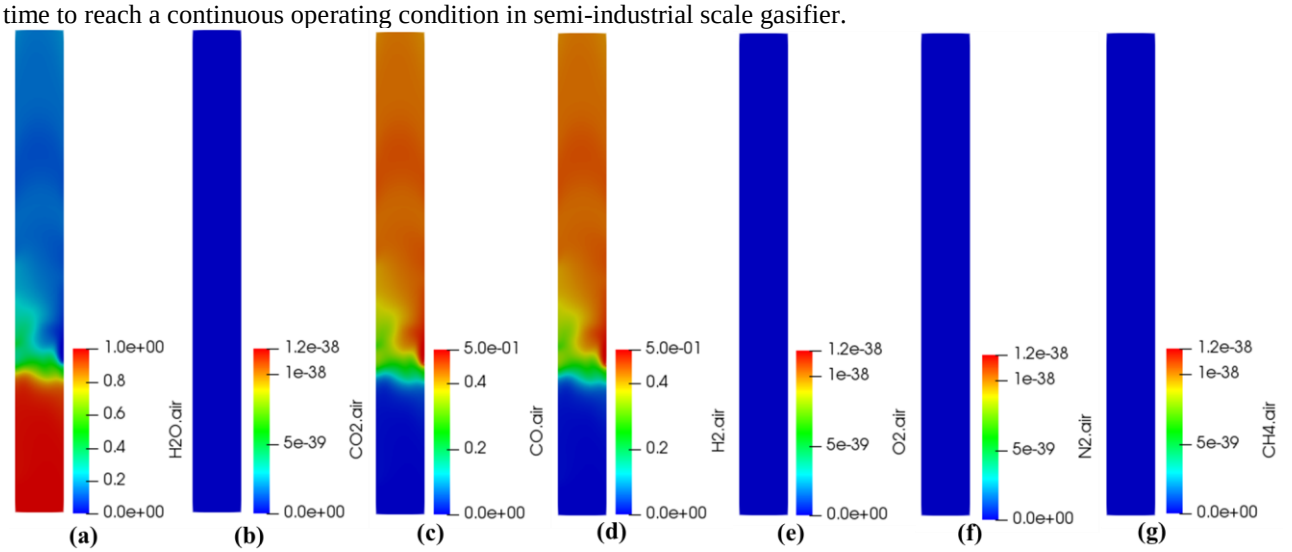

Figure 10. Final composition of the reactor at Reforming of char reaction simulation. (a) H_2O, (b) CO_2, (c) CO, (d) H_2, (e) O_2, (f) N_2 and (g) CH_4.

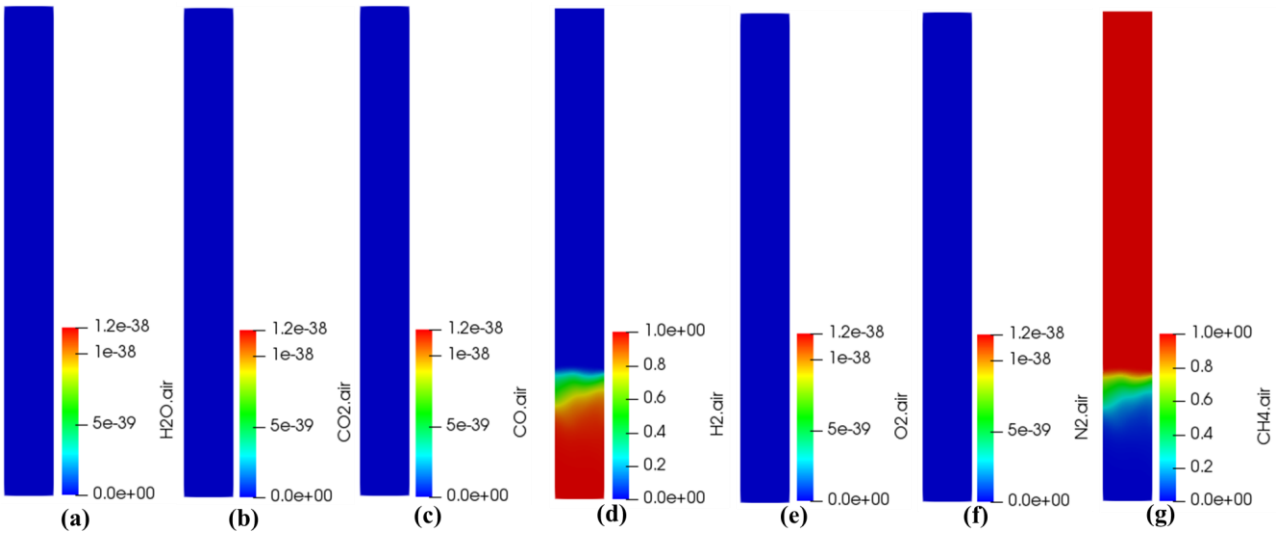

Figure 11. Final composition of the reactor at Methanation reaction simulation. (a) H_2O, (b) CO_2, (c) CO, (d) H_2, (e) O_2, (f) N_2 and (g) CH_4.

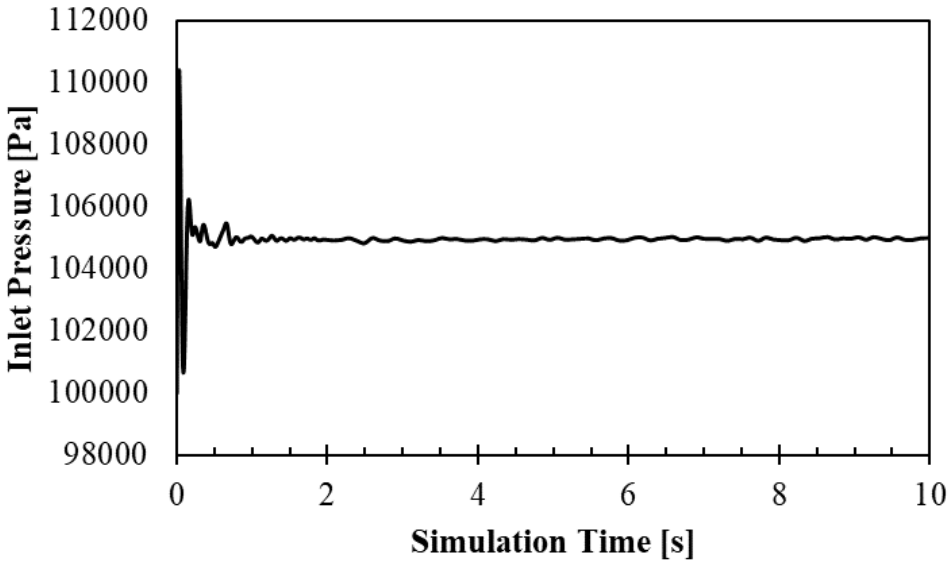

Figure 12. Inlet pressure over simulation time

4. CONCLUSIONS

This work was focused on the evaluation of a CFD implementation of chemical heterogeneous reactions, which consist of the main reactions present at the gasification process. It was verified the possibility of the implementation of any heterogeneous reactions, which can even include combustion reactions within Eulerian-Eulerian approach.

The simulations allowed to infer relevant information about the functionality of the thermochemical reactor, as ones related to the reacting zone and time for fluid-dynamic and chemical stabilization. The chemical reactions implementation provides consistent results in representing the consumption of char particles, the reacting with the gaseous agent and the production of other species. The mass transfer between phases was also satisfied and the energy source term of each chemical reaction well arranged into the fluid-dynamic system.

The implementation conducted in the present work is part of a development of a fully CFD model to represent a semi-industrial scale gasifier of the research line of the authors group.

5. ACKNOWLEDGEMENTS

The authors are grateful for the financial support provided by Agência Financiadora de estudos projetos (FINEP-ROTA2030), Coordenação de Aperfeiçoamento de Pessoal de Nível Superior (CAPES), Conselho Nacional de Desenvolvimento Científico e Tecnológico (CNPq), and Fundação de Amparo à Pesquisa do Estado de Minas Gerais (FAPEMIG).

6. REFERENCES

Chase, M.W., 1998. "NIST-JANAF Thermochemical Tables, 4th Ed. J. Phys. Chem. Ref. Data. 1998, Monograph 9(Part I and Part II)". *Journal of Physical and Chemical Reference Data*. p. Part I&II.

Ergun, S., 1952. "Fluid Flow through Packed Columns".

Gidaspow, D., 1994. *Multiphase Flow and Fluidization: Continuum and Kinetic Theory Descriptions*. *Multiphase Flow and Fluidization: Continuum and Kinetic Theory Descriptions*.

Hasse, C., Debiagi, P., Wen, X., Hildebrandt, K., Vascellari, M. and Faravelli, T., 2021. "Advanced modeling approaches for CFD simulations of coal combustion and gasification". *Progress in Energy and Combustion Science*. 86(June), p. 100938.

Infiesta, L.R., Ferreira, C.R.N., Trovó, A.G., Borges, V.L. and Carvalho, S.R., 2019. "Design of an industrial solid waste processing line to produce refuse-derived fuel". *Journal of Environmental Management*. 236(1), pp. 715–719.

Kakaç, S. and Pramuanjaroenkij, A., 2009. "Review of convective heat transfer enhancement with nanofluids". *International Journal of Heat and Mass Transfer*. 52(13–14), pp. 3187–3196.

Klimanek, A. and Bigda, J., 2018. "CFD modelling of CO2 enhanced gasification of coal in a pressurized circulating fluidized bed reactor". *Energy*. 160, pp. 710–719.

Ku, X., Li, T. and Løvås, T., 2015. "CFD-DEM simulation of biomass gasification with steam in a fluidized bed reactor". *Chemical Engineering Science*. 122, pp. 270–283.

Ranz, W.E. and Marshall, W.R., 1952. "Evaporation from drops". *Chem. Eng. Progr*. 48(22), pp. 141–173.

Rusche, H., 2002. "Computational Dispersed Two-Phase Dynamics Flows of At Phase Fractions". (1).

Sutherland, W., 1893. "The viscosity of gases and molecular force". *The London, Edinburgh, and Dublin Philosophical Magazine and Journal of Science*. 36(223), pp. 507–531.

Wen, C.Y. and Yu, Y.H., 1966. "A generalized method for predicting the minimum fluidization velocity". *AIChE Journal*. 12(3), pp. 610–612.

Zhong, W., Yu, A., Zhou, G., Xie, J. and Zhang, H., 2016. "CFD simulation of dense particulate reaction system: Approaches, recent advances and applications". *Chemical Engineering Science*. 140, pp. 16–43.

7. RESPONSIBILITY NOTICE

The authors are the only responsible for the printed material included in this paper.